

DOI: 10.31534/engmod.2020.3-4.ri.07m

Professional paper

Received: 31.05.2020.

Interfacial Bond Adhesion Enhancement Mechanism Analysis of Self Stressing Alkali Activated Slag Concrete-Filled Round Steel Tube

Xiaohui Yuan^(*), Yongqiang Li, Shige Wang

College of Architecture and Civil Engineering, Xinyang Normal University, Xinyang 464000, CHINA

e-mail: yxiaohui2006@163.com

SUMMARY

To investigate the interfacial adhesion behaviour and its enhancement mechanism of self-stressing alkali activated slag concrete-filled round steel tube, push-out samples, expansion performance test specimens, and SEM, XRD micro-test specimens were made with different dosage of calcium sulphoaluminate and calcium oxide expansive agent. The results show that the maximum interfacial adhesion stress is at 70-80 mm from the free end of the samples, and increases with the increase of the expansive agent dosage. The expansive agent such as calcium sulphoaluminate and calcium oxide can effectively reduce the drying shrinkage performance of the core concrete, and then improve the interaction between steel tube and core concrete. Micro-test analysis results show that the main expansive source providing expansive power in the AASC system is Ca(OH).

KEY WORDS: *self-stressing; alkali activated slag concrete (AASC); interfacial adhesion strength; expansive resources.*

1. INTRODUCTION

With such advantages as environmental protection, fast hardening, early strength, and storage resistance [1-2], Alkali-activated slag concrete (AASC) has been well applied in the civil engineering industry. In the concrete-filled steel tube (CFST) structure, a steel tube can be used as a concrete form, which can increase the construction speed [3]. The AASC and steel tube are combined to form an AASC-filled steel tube structure, fully utilizing the advantages of fast material hardening and convenient construction of steel tube concrete. This new material structure can be applied to emergency repair projects. For the CFST structure, one important precondition is to ensure good adhesion behaviour between the steel tube and the core concrete. However, the concrete has the characteristics of volume shrinkage, and especially for

the AASC concrete, its volume shrinkage is higher than that of ordinary concrete [4], which will cause the interface between steel tube and concrete to be debonded or disengaged. At present, in view of this problem, the expansive agent is usually added into the concrete to produce the dilatants such as ettringite [5-6], $Ca(OH)_2$ [7] or $Mg(OH)_2$ [8] and reduce the drying shrinkage of the concrete, or expand its volume to produce self-stressing. Therefore, the addition of an expansive agent to the CFST can reduce the interface defects between the steel tube and the concrete to a certain extent, and increase the interaction between the two, thereby improving the interfacial adhesion.

In the current researches on the interfacial adhesion behaviour between steel tubes and concrete, the push-out tests and push-off tests have been mostly adopted by many scholars. As early as 1975, Viridi and Dowling [9] conducted the push-out experiment to study the influence of core concrete strength, section size, interface roughness and contact length on the interfacial adhesion strength of concrete-filled steel tube. The results showed that the mechanical interaction of interface is the main factor affecting the interface adhesion strength. In 2006, Liu Yongjian [10], using the push-out test, studied the distribution law of the CFST interfacial adhesion strength along with the member length, concluding that it's triangular-distributed. In 2009, Chang and Huang et al. [11] studied the interfacial adhesion strength of self-stressing CFST through push-out experiments and found that its interfacial adhesion strength is about 1.2-3.3 times higher than that of ordinary CFST. In 2018, Zheng Liang et al. [12] carried out the test about the interfacial adhesion behaviour of CFST under high stress; the test results showed that the interfacial stress is high under high-stress state, and the expansive agent has a large effect on interfacial adhesion stress, but its influence mechanism wasn't analysed.

Based on the above analysis, this paper studies the interfacial adhesion behaviour of the AASC-filled steel tube with the dosage of the expansive agent as the variable. Also, it conducts micro-test analysis for the enhancement mechanism of the interfacial adhesion strength doped with the expansive agent. The relevant research results are expected to provide a theoretical reference for structural design and engineering practice.

2. INTERFACIAL ADHESION STRENGTH FUNCTION

During the entire push-out test, it's assumed that the steel tube and the core concrete are always in an elastic phase, with the stress uniformly and continuously distributed. The core concrete inside the test micro-section was taken as the research object. Figure 1 shows the stress balance diagram of the micro-section, and Formula (1) lists the equilibrium equation. The interfacial adhesion force $\tau(x)$ was balanced with the force between the steel tube and the core concrete. Then, taking the unit length for force analysis, the equilibrium relation was obtained as shown in Formula (2).

$$\tau(x) = \frac{\Delta N}{l_s \cdot dx} = \frac{A_c \cdot d\sigma_c}{l_s \cdot dx} = \frac{D-2t}{4} \cdot E_c \cdot \frac{d\varepsilon_c}{dx} = \frac{D_0}{4} \cdot E_c \cdot \frac{d\varepsilon_c}{dx} \quad (1)$$

$$A_s E_s d\varepsilon_s + A_c E_c d\varepsilon_c = 0 \quad (2)$$

Let $E_c/E_s = \alpha_E$, $A_c/A_s = \beta_A$,

then:

$$d\varepsilon_c = -\alpha_E \cdot \beta_A \cdot d\varepsilon_s \quad (3)$$

where: l_s is the inner wall circumference of the steel tube; l_a is the interfacial bonding length; D is the outer diameter of the tube; D_0 is the inner diameter of the tube; E_s, E_c are the elastic modulus of the steel tube and the core concrete respectively; A_s, A_c are the cross-sectional area of the steel tube and the core concrete; $\varepsilon_s, \varepsilon_c$ are the strain of the steel tube and the core concrete respectively.

According to the relevant boundary conditions, substituting the Formula (3) into (1), the interfacial adhesion stress can be expressed as:

$$\tau(x) = \begin{cases} 0 & x = 0 \\ \frac{D_0}{4} \cdot E_s \cdot \beta_A \cdot \frac{d\varepsilon_s}{dx} & 0 < x < l_a \\ 0 & x = l_a \end{cases} \quad (4)$$

The literature [13-14] suggests that the steel tube surface strain along the sample length direction under different load levels is negatively exponentially distributed during the push-out test, so the steel surface strain gauge can be placed at different heights of the test specimen during the test, to obtain the strain distribution on the surface of the steel tube during the pushout process. Besides, the negative exponential function can be used to fit the strain curve under different load levels. After substituting the final fitting function into the Formula (4), we can obtain the correspondence relationship between interfacial adhesion strength and position of test specimens.

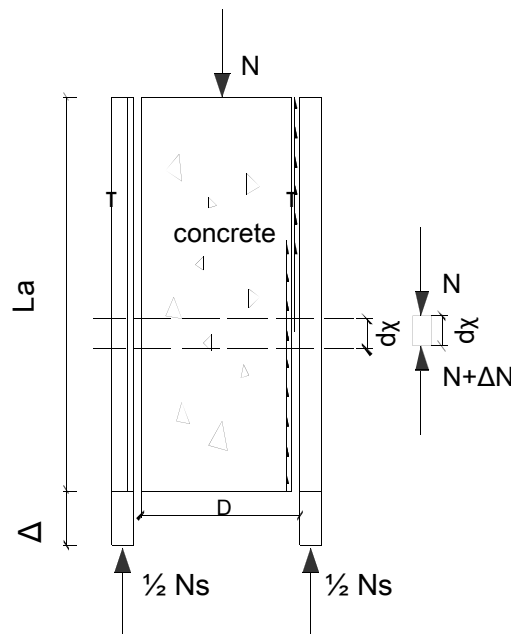


Fig. 1 Stress balance of micro-sections

3. INTERFACIAL ADHESION STRENGTH TEST

3.1 RAW MATERIALS

Cementitious material: WISCO mineral powder (slag), with moisture content 13.2 %, density 3.051 g/cm³, and grade S95. Activator: water glass, in molecular formula Na₂O·nSiO₄, with modulus 3.03, and solid content 37.5; commercially available NaOH at the purity of 99.8 %; clean tap water; the activator was formed by mixing the water glass, NaOH and water according to mass ratio (NaOH: water glass: water=1.0: 8.1: 5.0). Expansive agent (EA): calcium sulphoaluminate-calcium oxide expansive agent, with CaO content of 60.64 %. Coarse aggregate: stone with a particle size of 5-35 mm and a crushing value of 11.8. Fine aggregate: river sand, fineness modulus 2.72, belonging to medium sand. Steel tube: the diameter of steel tube was selected to be $D \times \text{thickness } t \times \text{height } L = 165 \text{ mm} \times 3 \text{ mm} \times 495 \text{ mm}$, and the steel tube was welded straight seam of the tube.

3.2 SPECIMEN PRODUCTION

There were three groups of test specimens, 2 specimens in each group, and a total of 6 specimens. The dosage of the expansive agent in each group was 0 %, 4 %, and 6 %, respectively. The AASC mix ratio is shown in Table 1. During the production process of specimens, the concrete pouring was carried out by layering, and each time 1/3 the height of the test specimen was poured. The pouring was completed three times. After each pouring, the mechanical vibrating rod was used to vibrate and compact, and the core concrete was levelled to ensure the same height with the steel pipe. Afterward, it was sealed with plastic wrap and cured for 28 days in a standard curing room at a temperature of 20±3°C and relative humidity of 95 %.

Table 1 Concrete mix ratio

Group	No.	Slag (Kg)	Coarse aggregate (Kg)	Fine aggregate (Kg)	Activator (Kg)	Ratio of solution to adhesive	EA (kg)	EA (%)
1	IBC0-1	400	1126.4	633.6	232.7	0.58	0	0%
	IBC0-2	400	1126.4	633.6	232.7	0.58	0	0%
2	IBC4-1	384	1126.4	633.6	232.7	0.58	16	4%
	IBC4-2	384	1126.4	633.6	232.7	0.58	16	4%
3	IBC6-1	368	1126.4	633.6	232.7	0.58	24	6%
	IBC6-2	368	1126.4	633.6	232.7	0.58	24	6%

3.3 MEASURING POINT ARRANGEMENT AND LOADING SCHEME

According to the theoretical analysis above, the longitudinal strain gauges were arranged along the surface of the steel tube at a distance of 70 mm. Figure 2 shows the specific layout position. The stiffener was added near the free end to avoid excessive deformation of the steel tube during the test and affecting the test results. With displacement loading, the loading rate was controlled at 0.02 mm/s, and finally the push-out displacement of 30 mm or more means that the core concrete is pushed out. Figure 3 depicts the diagram of the test device.

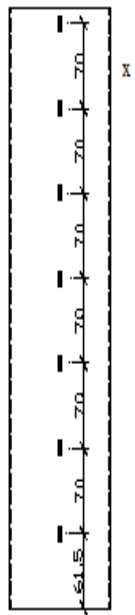


Fig. 2 Measuring point layout

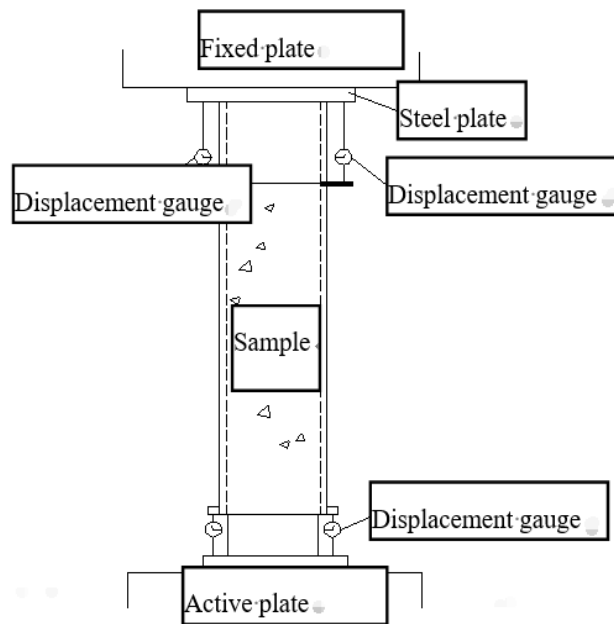
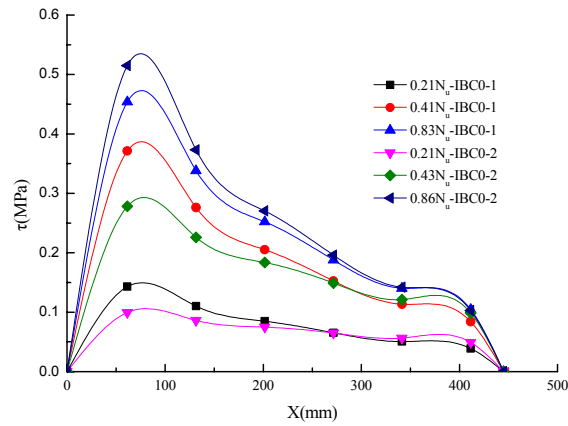


Fig. 3 Test devices

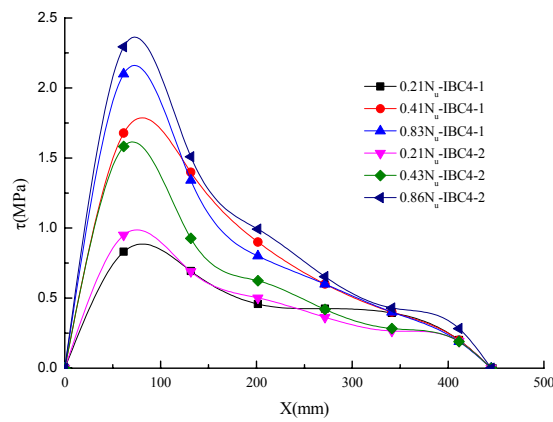
3.4 TEST RESULTS OF INTERFACE ADHESION STRENGTH

According to the surface longitudinal strain test results of the steel tube, the relationship between the longitudinal strain and the corresponding position under different loads was fitted by the negative exponential function $\varepsilon_s(x)$ using MATLAB software. Then, the fitting function was substituted into the Formula (4) to obtain the correspondence between the interfacial adhesion stress and the height of the test specimen (Figure 4). In the figure, N_u is the push-out limit load, the coefficient before N_u is the ratio of the load N at each level to the push-out limit load N_u , and IBCm-n ($m=0, 4, 6, n=1, 2$) is the No. test specimen of concrete dosed with m % expansive agent.

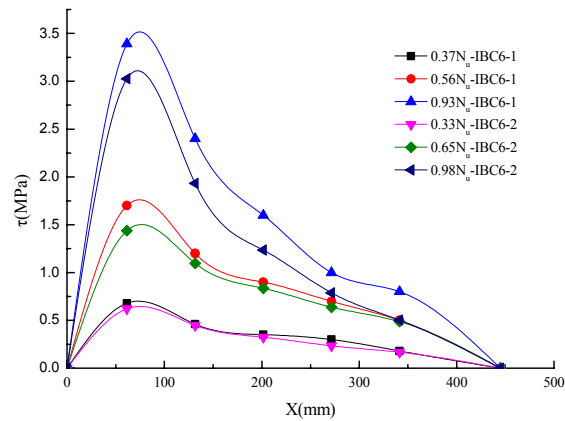
It can be seen from Figure 4 that the maximum interfacial adhesion stress of each specimen occurs about 70-80 mm from the free end, and it increases with the increase of the expansive agent content. The maximum adhesion stress is about 0.5 MPa with 0 % expansive agent; with 4 % dosage of the expansive agent, it is about 2.2 MPa; with 6 %, it is obviously increased to 3.2 MPa.



(a) IBC0



(b) IBC4



(c) IBC6

Fig. 4 Distribution of interfacial adhesion strength of every specimen with its height

4. ENHANCEMENT MECHANISM ANALYSIS OF INTERFACIAL ADHESION STRENGTH

The interfacial adhesion stress between the steel tube and the core concrete is mainly composed of chemical adhesive force, friction force, and mechanical interaction. The chemical adhesive force is very small, and it will be lost under the action of tiny load; the friction is

mainly generated in the presence of the radial pressing force between the steel tube and the core concrete; the mechanical interaction is mainly caused by the uneven inner surface of the steel tube. For the steel tube, even with the relatively smooth inner surface, the mechanical interaction is still not obvious. Therefore, the friction force plays the main role in the interfacial adhesion strength between the steel tube and the core concrete. Under the push-out load, the core concrete will produce lateral deformation, while the outer steel tube will constrain the lateral expansion of the core concrete. This interaction provides the main compressive stress on the interface to produce the bond stress. For self-stressing CFST, the addition of the expansive agent causes the core concrete to expand in volume or extrudes a steel tube to produce the self-stress, which can increase the compressive stress between the steel tube and the core concrete. However, it is unclear how the expansive agent improves the volumetric shrinkage of the core concrete and what expansive source is used for that. Therefore, in this paper, related research in this area was carried out.

4.1 EXPANSIVE PERFORMANCE TEST OF CORE CONCRETE

The specimens of a size of $165 \times 495 \times 4$ (mm) were tested by a custom expanding rate tester. The dosage of the expansive agent was increased by 2 % and 8 % respectively. The test temperature was controlled at $23 \pm 1^\circ\text{C}$ and the humidity was at about 40 %. Figure 5 shows the expansive performance test chart of the core concrete.

Figure 6 shows the time history curve of the shrinkage ratio for the core concrete under different expansive agent dosages. It can be seen from the figure that the addition of the expansive agent can effectively improve the shrinkage ratio of the core concrete, and its shrinkage mainly occurs within the first 7 days. With 0 % expansive agent, the drying shrinkage of the core concrete was about $4.4 \times 10^{-4} \mu\epsilon$; With the expansive agent added, the shrinkage ratio of the core concrete was reduced to about $0.5 \times 10^{-4} \mu\epsilon$, and the shrinkage effect was obvious, specifically, when the dosage of expansive agents increased from 2 % to 8 %, the drying shrinkage ratio declines insignificantly. The stable dry shrinkage rate for the dosage of 2 %, 4 %, 6 %, and 8 % expansive agent was $0.52 \times 10^{-4} \mu\epsilon$, $0.42 \times 10^{-4} \mu\epsilon$, $0.41 \times 10^{-4} \mu\epsilon$ and $0.38 \times 10^{-4} \mu\epsilon$. Thus, the incorporation of the expansive agent greatly reduces the shrinkage of the core concrete. During the push-out test, under the push-out load, the compressive stress between the steel tube and the core concrete gradually increases with the increase of the expansive agent dosage, which improves the interfacial adhesion between the two.

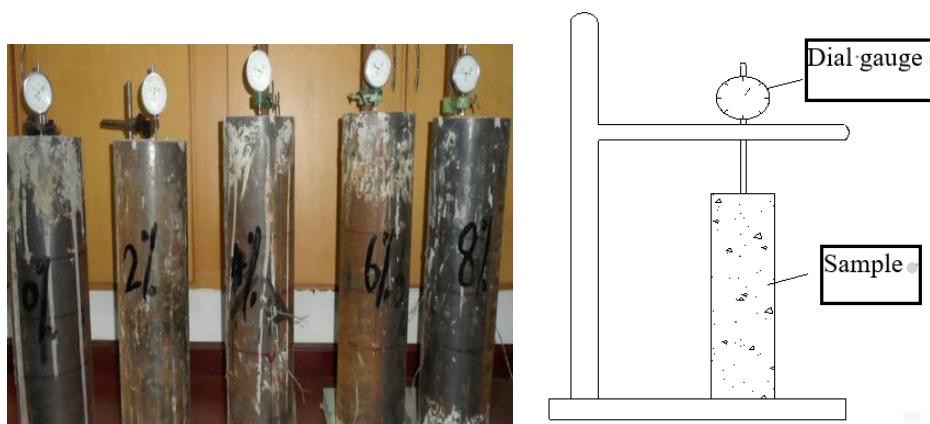


Fig. 5 Expansive performance test of core concrete

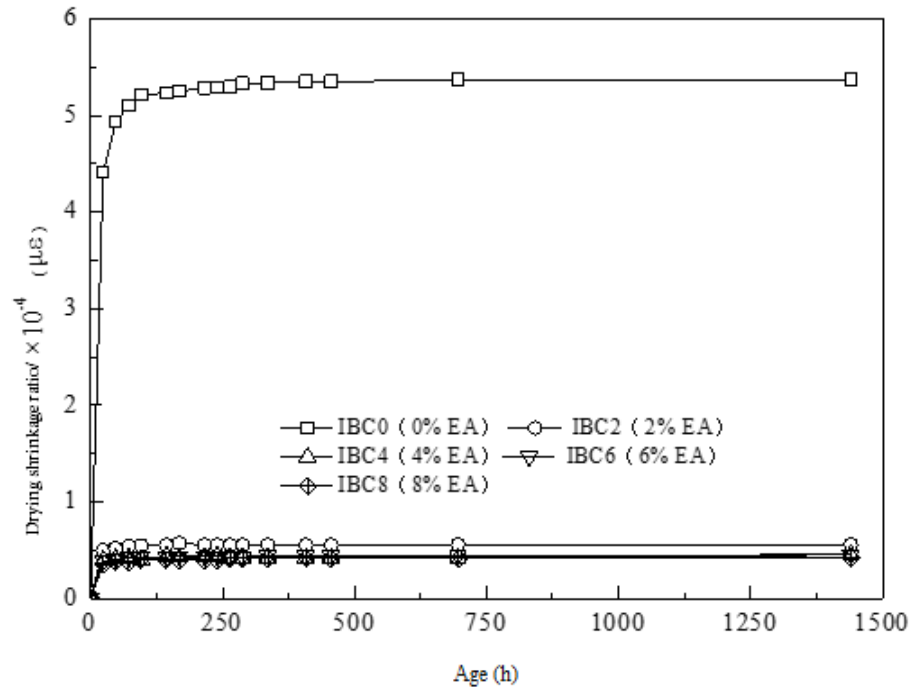


Fig. 6 Drying shrinkage ratio of core concrete with different dosages of expansive agents

4.2 EXPANSIVE SOURCE TEST

The expansion principle of calcium sulphoaluminate-calcium oxide expansive agent is to form a plate-like or flake-like $Ca(OH)_2$ crystal by calcium oxide reaction as an expansive source in the early stage and to provide expansion power by promoting the formation of calcium vanadium in the later stage. Under normal circumstances, if the dosage of calcium sulfate in the raw material is sufficient, the trisulfate type calcium sulphoaluminate is formed, and its chemical formula is $3CaO \cdot Al_2O_3 \cdot 3CaSO_4 \cdot 30-32H_2O$, also known as calcium vanadium, wherein aluminum can be replaced by iron, abbreviated as AFt. If the calcium sulfate content is small, a mono-sulfate type calcium sulphoaluminate AFm is formed, and the chemical formula is $3CaO \cdot Al_2O_3 \cdot CaSO_4 \cdot nH_2O$, where the most common one is $3CaO \cdot Al_2O_3 \cdot CaSO_4 \cdot 12H_2O$, and its crystal is a pseudo hexagonal plate shape or a needle tip shape.

Figure 7 shows the SEM image of the core concrete slurry on the 7d, in which the plate or sheet-like $Ca(OH)_2$ crystal formation can be clearly seen in the samples with 4 % and 6 % expansive agent dosage, except the sample with 0 % expansive agent.

Figure 8 shows the XRD pattern of the core concrete on the 7d, where the peak of the $CaCO_3$ crystal is clearly visible in the spectrum. There is no peak of $Ca(OH)_2$ crystal in the sample with 0 % expansive agent, but with the expansive agent dosage increased from 4 % to 6 %, the peak of the $Ca(OH)_2$ crystal is increasingly obvious.

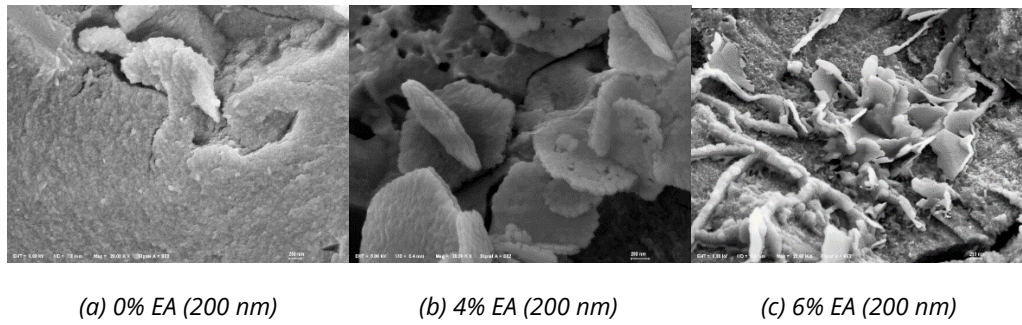


Fig. 7 SEM image of core concrete slurry on the 7d

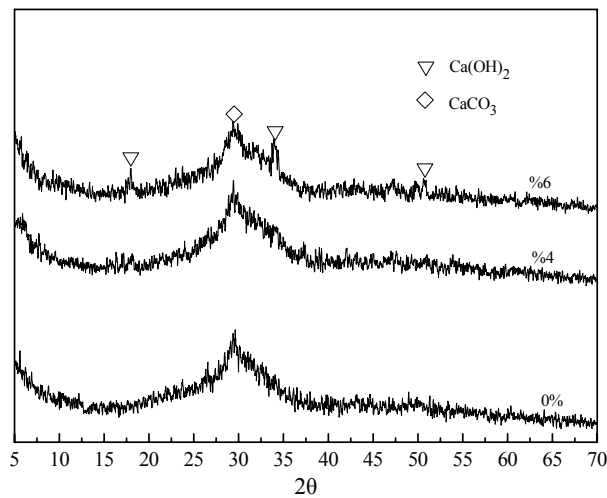


Fig. 8 XRD pattern of core concrete slurry on the 7d

According to the micro-test analysis of SEM and XRD, it's found that the hydration product Ca(OH)_2 is the main provider for expansive power in the core concrete after the expansive agent is added, but there is no ettringite created in the hydration product. Based on the research conclusions of Khan and Kayali [15], Gu Yamin et al. [16], the reason for failing to form ettringite crystal is mainly that in the AASC system, too high OH^- ion concentration reduces the concentration of Ca^{2+} , SO_4^{2-} which is necessary for the formation of ettringite crystals.

The above analysis shows that the production of Ca(OH)_2 hydration product after the addition of the expansive agent can compensate for the volume shrinkage of the core concrete and increase the interaction between the core concrete and the steel pipe. According to the formation mechanism of ettringite and the conclusions from the literature [15] and [16], as the age increases, it is difficult for core concrete to form a more stable ettringite product. Ca(OH)_2 is extremely unstable when exposed to air, easily forming CaCO_3 . However, the core concrete in the AASC of round steel hardly comes into contact with the environment, so for the internal Ca(OH)_2 is difficult to become carbonized. The addition of an expansive agent can increase the interfacial adhesion behavior between the steel pipe and the AASC, but the content is not recommended to exceed 8 %, because it's found during the test that the concrete performance drops sharply after 8 %, and it is difficult to form.

5. CONCLUSIONS

- (1) The maximum interfacial adhesion stress of a self-stressing concrete-filled round steel tube occurs at 70-80 mm from the free end. With the increase of the expansive agent dosage, the interfacial adhesion stress increases gradually.
- (2) The incorporation of the expansive agent such as calcium sulphoaluminate and calcium oxide can effectively improve the drying shrinkage performance of core concrete in AASC-filled steel tube, and the shrinkage ratio of core concrete can be reduced by about $3.9 \times 10^{-4} \mu\epsilon$.
- (3) With the Calcium sulphoaluminate-calcium oxide type expansive agent added, the hydration product $Ca(OH)_2$ shall be the main provider of the expansion power in AASC.
- (4) The addition of calcium sulfoaluminate expansive agent is conducive to improving the interface adhesion between the steel pipe and AASC, but the dosage (according to the internal admixture method) is recommended not to exceed 8 %.

6. REFERENCE

- [1] X.H. Yuan, X.W. Shen, Experimental study on shrinkage compensation performance of alkali-activated slag concrete, *Bulletin of the Chinese Ceramic Society*, Vol. 36, No. 9, pp. 2987-2993, 2017.
- [2] H. Xie, J.C. Liu, S.J. Hou, Experimental study on sound absorption performance of alkali activated slag cement foam concrete, *Bulletin of the Chinese Ceramic Society*, Vol. 36, No. 8, pp. 2775-2780, 2017.
- [3] L.H. Han, Z. Tao, W. Liu, Concrete filled steel tubular structures from theory to practice, *Journal of Fuzhou University (Natural Science)*, No. 6, pp. 24-34, 2001.
<https://doi.org/10.3969/j.issn.1000-2243.2001.06.004>
- [4] F. Collins, J.G. Sanjayan, Effect of pore size distribution on drying shrinkage of alkali-activated slag concrete, *Cement and Concrete Research*, Vol. 30, No. 9, pp. 1401-1406, 2000. [https://doi.org/10.1016/S0008-8846\(00\)00327-6](https://doi.org/10.1016/S0008-8846(00)00327-6)
- [5] H. Lafuma, Expansive cement, Proc. 3rd ISCC, London, UK, *Cement and Concrete Association*, pp. 581-596, 1952.
- [6] W. Chen, H.J.H. Brouwers, Hydration of mineral shrinkage-compensating admixture for concrete: an experimental and numerical study, *Construction and Building Materials*, Vol. 26, No. 1, pp. 670-676, 2012. <https://doi.org/10.1016/j.conbuildmat.2011.06.070>
- [7] S. Nagataki, H. Gomi, Expansive admixtures (mainly entering), *Cement and Concrete Composites*, Vol. 20, No. 2-3, pp. 163-170, 1998.
[https://doi.org/10.1016/S0958-9465\(97\)00064-4](https://doi.org/10.1016/S0958-9465(97)00064-4)
- [8] M.R. Nokken, Expansion of MgO in cement pastes measured by different methods, *ACI Materials Journal*, Vol. 107, No. 1, pp. 80-84, 2010. <https://doi.org/10.14359/51663469>
- [9] K.S. Viridi, P.J. Dowling, Bond strength in concrete filled circular steel tubes, CESLIC Report CC11, London: Engineering Structures Laboratories, *Civil Engineering Department, Imperial College*, 1975.

- [10] Y.J. Liu, J.J. Chi, Push-out test on shear bond strength of CFST, *Industrial Construction*, No. 4, pp. 78-80, 2006.
- [11] X. Chang, C.K. Huang, D.C. Jiang, Push-out test of pre-stressing concrete filled circular steel tube columns by means of expansive cement, *Construction and building materials*, Vol. 23, No. 1, pp. 491-497, 2009. <https://doi.org/10.1016/j.conbuildmat.2007.10.021>
- [12] L. Zheng, D.P. Zhang, H. Guo, S.M. Yan, L. Wang, Y.L. Wu, Research on Bond Behavior of Concrete Filled Steel Tube under High Stress, *Journal of Zhengzhou University (Engineering Science)*, Vol. 39, No. 01, pp. 18-23, 2018.
- [13] Y.L. Xu, Experimental research on bonding and anchoring behavior of deformed reinforced steel concrete, 1990.
- [14] X.L. Kang, Study on compositing mechanical performance and bond-slip performance of concrete filled steel tube, 2007.
- [15] M.S.H. Khan, O. Kayali, Effect of NaOH activation on ettringite in concrete containing ground granulated blast furnace slag, *Third International Conference on Sustainable Construction Materials and Technologies*, pp. 1-11, 2013. <https://doi.org/10.1088/1475-7516/2017/04/007>
- [16] Y.M. Gu, Y.H. Fang, Shrinkage, Cracking, Shrinkage-Reducing and Toughening of Alkali-Activated Slag Cement-A Short Review, *Journal of the Chinese Ceramic society*, Vol. 40, No. 1, pp. 76-84, 2012.